



Contents lists available at ScienceDirect

## Advanced Powder Technology

journal homepage: [www.elsevier.com/locate/apt](http://www.elsevier.com/locate/apt)

Original Research Paper

Hydrothermal synthesis of NH<sub>2</sub>-UiO-66 and its application for adsorptive removal of dyeSneha N. Tambat<sup>a</sup>, Priyanka K. Sane<sup>a</sup>, Srinidhi Suresh<sup>a</sup>, Nilesh Varadan O.<sup>a</sup>, Aniruddha B. Pandit<sup>a</sup>, Sharad M. Sontakke<sup>a,b,\*</sup><sup>a</sup> Department of Chemical Engineering, Institute of Chemical Technology, Mumbai 400019, India<sup>b</sup> Department of Chemical Engineering, Birla Institute of Technology and Science, Pilani, K K Birla Goa Campus, Goa 403726, India

## ARTICLE INFO

## Article history:

Received 2 June 2018

Received in revised form 9 July 2018

Accepted 19 July 2018

Available online xxxxx

## Keywords:

NH<sub>2</sub>-UiO-66

Adsorption

Safranin

Kinetics

Isotherm

## ABSTRACT

In this research paper we report hydrothermal synthesis of NH<sub>2</sub>-UiO-66, a metal organic framework (MOF) with zirconium as metal and amino terephthalic acid as a linker. The synthesized MOF was characterized by XRD, FTIR, SEM and BET surface area. As a potential application in water treatment, an adsorptive removal of safranin dye was studied using the synthesized material. The effect of initial concentration and pH of the dye solution was studied on the dye adsorption capacity of the material. An optimum set of conditions resulting into maximum dye adsorption was found out. The maximum adsorption capacity of the MOF was observed to be 390 mg/g at neutral pH of the solution and at room temperature. The experimental data was fitted with Langmuir, Freundlich and Temkin adsorption isotherm models. The kinetics of adsorption was studied using pseudo first order and pseudo second order model. The dye adsorption mechanism was also attempted.

© 2018 The Society of Powder Technology Japan. Published by Elsevier B.V. and The Society of Powder Technology Japan. All rights reserved.

## 1. Introduction

Metal organic frameworks (MOFs) are a class of advanced porous, crystalline materials synthesized from organic linkers and transition metal ions (or clusters) [1]. These materials are receiving increasing scientific attention for variety of applications owing to their ease of synthesis, high surface area, high porosity, high thermal and mechanical stability, tunable structural and functional properties, etc. [1,2].

The MOFs have been extensively investigated as an adsorbent for the treatment of polluted water [3,4]. However, most of these materials are unstable in water and subject to degradation through ligands displacement or hydrolysis [4]. Among the reported MOFs, UiO-66 and NH<sub>2</sub>-UiO-66 (UiO = University of Oslo) exhibit high stability in water and have excellent adsorption properties [4,5] because of which these are receiving considerable attention for adsorptive removal of water pollutants [4,6–8].

Residual synthetic dyes, in the effluent of textile, leather, paper, printing, cosmetics, petroleum, plastic, food, paint, rubber, and pharmaceutical industries are the major contributor to water

pollution [9,10]. Many of these chemical pollutants are identified as mutagenic, carcinogenic and if consumed in excess quantity can cause severe damage to human health [11]. In addition, the water contaminated with these chemicals can be a potential threat to aquatic life [12]. Therefore, majority of the research in the field of water treatment is focused on removal of dye pollutants. Several conventional and advanced oxidation techniques are reported for the removal of these pollutants [13–16]. Among the available techniques, adsorption is an economical yet efficient method for the removal of variety of synthetic dyes [6,17]. In this context, a considerable amount of literature is available on variety of adsorbents including activated carbon, diatomaceous earth, resins, zeolites, carbon nanotubes, etc. In general, a good adsorbent should possess high surface area, high porosity, ease of synthesis, less cost, high thermal and mechanical properties, regeneration ability and high adsorption capacity towards a wide range of pollutants within a short contact time [6,18]. Since UiO-66, NH<sub>2</sub>-UiO-66 and few other MOFs satisfy most of the above requirements; these are considered to be potential alternative adsorbents for the treatment of dye polluted water.

Chen and coworker studied the adsorptive removal of various anionic and cationic dyes using UiO-66 and NH<sub>2</sub>-UiO-66 MOF [6]. They observed superior adsorption of cationic dyes on to the NH<sub>2</sub>-UiO-66 compared to UiO-66. A microwave-assisted synthesis

\* Corresponding author at: Birla Institute of Technology and Science, Pilani, K K Birla Goa Campus, Goa 403726, India.

E-mail address: [sharads@goa.bits-pilani.ac.in](mailto:sharads@goa.bits-pilani.ac.in) (S.M. Sontakke).

<https://doi.org/10.1016/j.apt.2018.07.010>

0921-8831/© 2018 The Society of Powder Technology Japan. Published by Elsevier B.V. and The Society of Powder Technology Japan. All rights reserved.

of UiO-66 and its application for the adsorptive removal of acid chrome blue K is reported by Li and coworkers [8]. He and coworker reported adsorptive removal of Rhodamine B on UiO-66 [19]. They observed increase in the adsorption capacity with temperature and the maximum dye adsorption capacity was observed to be about 75 mg/g at 323 K. They also studied the regeneration of the spent adsorbent and demonstrated reuse of the material for six cycles of sorption/desorption. In another study, an adsorptive behavior of UiO-66 for the removal of acid orange 7 (AO7) dye was investigated and a maximum adsorption capacity of about 358 mg/g was observed at 318 K [20]. Recently, Embaby et al. studied adsorption of a series of anionic (Alizarin Red S, Eosin, Fuchsin Acid and Methyl Orange) and cationic (Neutral Red, Fuchsin Basic, Methylene Blue and Safranin T) dyes onto the UiO-66 and reported a record maximum adsorption capacity of 400 mg/g for adsorption of Alizarin Red S dye [21]. In literature, most of the studies are performed with UiO-66 however, application of NH<sub>2</sub>-UiO-66 for the adsorptive removal of dyes is least investigated.

The synthesis of MOFs is mainly reported by hydrothermal and microwave methods [6,8,19]. The hydrothermal method, under elevated temperature and pressure conditions, ensures complete solubilization of the organic molecules used as linker. These experimental conditions also help to overcome the activation energy required for intermediate metastable phases of synthesis and therefore, the synthesized material becomes highly crystalline [22,23]. The hydrothermally synthesized of UiO-66 family MOFs has been well reported in the literature. However, its application for dye adsorption is least investigated. For example, Shen and coworkers reported application of hydrothermally synthesis of NH<sub>2</sub>-UiO-66 for photocatalytic applications [24]. Luu and coworkers studied the application of NH<sub>2</sub>-UiO-66 for adsorption of CO<sub>2</sub> and CH<sub>4</sub> [25]. The only study available in the literature on application of hydrothermally synthesized NH<sub>2</sub>-UiO-66 for dye adsorption is reported by Chen and coworker [6]. In the above work, they reported adsorptive removal of three cationic dyes (Methylene Blue, Rhodamine B and Neutral Red) and two anionic dyes (Methyl Orange and Acid Chrome Blue K) using UiO-66 and NH<sub>2</sub>-UiO-66. They observed preferential adsorption for cationic dye onto the MOFs. However, in the above work, the experiments were carried out at 20 ppm and the equilibrium dye adsorption capacity is reported as 96 mg/g for adsorption of methylene blue dye. The authors (Chen and coworkers) have not studied the effect of initial dye concentration or pH and there was no attempt of optimizing the experimental conditions.

In the present study, we report hydrothermal synthesis of NH<sub>2</sub>-UiO-66 and its application for the removal of cationic Safranin dye. The effect of initial concentration and pH of the dye solution was studied on the dye adsorption capacity of the material. The experimental data was fitted with Langmuir, Freundlich and Temkin adsorption isotherm models. The dye adsorption mechanism was also attempted.

## 2. Experimental

### 2.1. Chemicals and materials

All the chemicals used in the experiments were of analytical grade and were used without any further purification. The chemicals used were Zirconium chloride (S.D. Fine Chemicals Limited, Mumbai), 2-amino terephthalic acid (Sigma Aldrich), N, N-dimethyl formamide (DMF) (S.D. Fine Chemicals Limited, Mumbai) and methanol (S.D. Fine Chemicals Limited, Mumbai). deionized (DI) water was used to prepare all the solutions.

### 2.2. Synthesis of NH<sub>2</sub>-UiO-66

In a typical synthesis of NH<sub>2</sub>-UiO-66, 2.17 g of 2-amino terephthalic acid and 3.8 g of Zirconium chloride was added to 36 mL of DMF. The mixture was stirred for 30 min. It was then transferred to a stainless steel teflon-lined autoclave and maintained at 120 °C for 24 h. The solid thus obtained was washed first with DMF and then repeatedly with methanol. Finally, the as-obtained solids was dried at room temperature and further in an oven kept at 150 °C for 4 h.

### 2.3. Characterization of the synthesized material

The synthesized material, NH<sub>2</sub>-UiO-66, was characterized by XRD, FTIR, SEM, Zeta potential analysis and BET surface area. A powder X-ray diffraction pattern was recorded on a Bruker D8 Advance X-ray diffractometer (Bruker, USA), with Cu K $\alpha$  radiation in a range of 10–90° at a scanning speed of 0.2 s/0.02°. The crystallite size was calculated using Scherrer's calculator. An FTIR spectrum was recorded on a Spectrum Two™ spectrometer (Perkin Elmer, USA) in the range of 4000 cm<sup>-1</sup> to 500 cm<sup>-1</sup>. The surface morphology of the as-synthesized material was studied by a scanning electron micrograph taken on a JEOL JSM-6380 SEM instrument (JEOL, Japan). Zeta potential analysis of the synthesized materials was performed using a Zetasizer instrument (Malvern Instruments, UK). The BET surface area was measured by nitrogen adsorption-desorption isotherm using a PMI BET sorptometer (BET-201AEL-20SEL, USA).

### 2.4. Batch adsorption experiments

Batch adsorption studies were performed using the synthesized material for the removal of Safranin dye from aqueous solution. Initially, a stock solution (1000 mL) of 1000 ppm of Safranin dye in DI water was prepared. A required concentration of the solution was prepared by diluting the stock solution. The observed error in the initial dye concentration of the solution was  $\pm 2$  ppm. To this solution, a pre-weighed amount of adsorbent was added and the suspension was stirred on a magnetic stirrer at room temperature conditions. For analysis, samples were withdrawn for the solution at a regular interval of time. The samples were centrifuged in a Optima™ MAX-XP centrifuge, (Beckman Coulter, USA) in order to remove the adsorbent material and absorbance of the supernatant solution was noted using a UV-Vis spectrophotometer (Cary 50 UV-Vis, USA). The concentration of the unknown solution was then determined with the help of a pre-plotted calibration curve between the concentration of known solutions and their corresponding absorbance values. The experiments were continued until a constant concentration of the dye was observed at least in 5 successive readings. This constant concentration was attributed to equilibrium concentration.

The amount of dye adsorbed on the adsorbent at different time,  $t$ , is represented by  $q_t$  and calculated by:

$$q_t = (C_0 - C_t) * \frac{V}{W} \quad (1)$$

where  $C_0$  is the initial concentration (in mg/L) of dye,  $C_t$  is the concentration (in mg/L) of dye at time,  $t$ ,  $V$  is the volume (in L) of the solution and  $W$  is the amount (in g) of adsorbent.

Further, the amount of adsorption at equilibrium,  $q_e$  (mg/g), was calculated by:

$$q_e = (C_0 - C_e) * \frac{V}{W} \quad (2)$$

where  $C_e$  is the equilibrium concentration (in mg/L) of dye. All other quantities on right side of the above equation have same meaning as that in Eq. (1).

The procedure for kinetic experiments was similar to the equilibrium studies. Samples were collected at specific time interval and the unknown concentration of dye was measured with the help of calibration curve.

### 3. Results and discussion

#### 3.1. Characterization of synthesized $\text{NH}_2\text{-UiO-66}$

Fig. 1 shows a XRD pattern of the synthesized material. The recorded pattern shows crystalline nature of the material and is in good agreement with the earlier reports [22,23]. The crystallite size calculated using Scherrer's calculator was found to be  $15 \pm 2$  nm. The FTIR spectrum of the synthesized MOF is shown in Fig. 2. From the figure, the presence of major peaks can be observed at a wavelength of  $3452\text{ cm}^{-1}$ ,  $3348\text{ cm}^{-1}$ ,  $2988\text{ cm}^{-1}$ ,  $1564\text{ cm}^{-1}$  and  $1378\text{ cm}^{-1}$ . The absorption bands at  $3452\text{ cm}^{-1}$  and  $3348\text{ cm}^{-1}$  are attributed to the asymmetric and symmetric vibration of N-H group [26]. The presence of distinct peak at  $2988\text{ cm}^{-1}$  can be attributed to the C-H stretching of the physisorbed DMF molecules [18,21,27]. Whereas, the two distinct peaks at  $1564\text{ cm}^{-1}$  and  $1378\text{ cm}^{-1}$  can

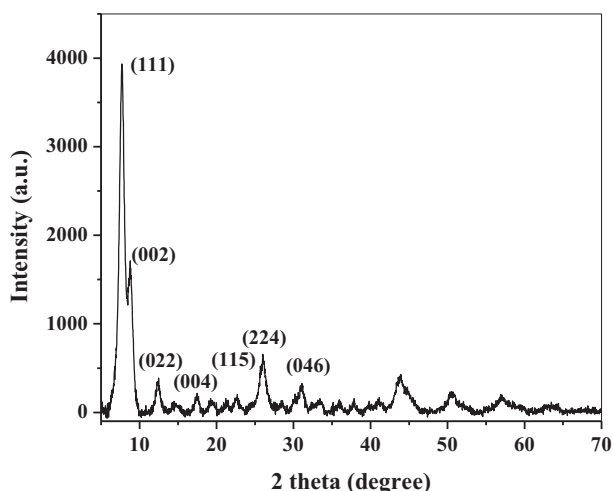


Fig. 1. XRD pattern of the synthesized  $\text{NH}_2\text{-UiO-66}$ .

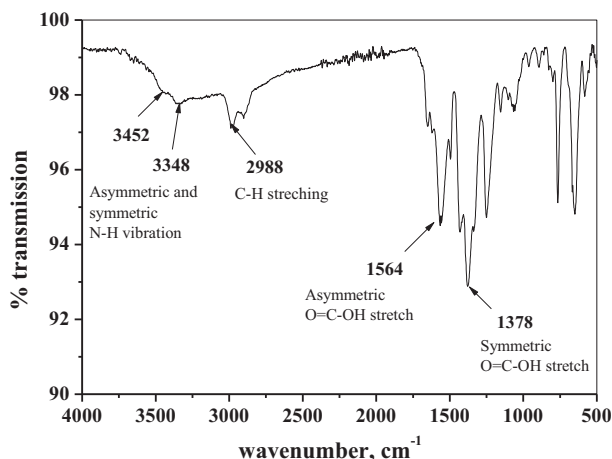


Fig. 2. FTIR spectrum of the synthesized  $\text{NH}_2\text{-UiO-66}$ .

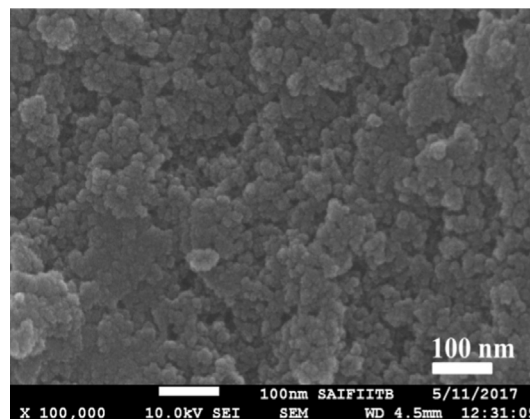


Fig. 3. SEM image of the synthesized  $\text{NH}_2\text{-UiO-66}$ .

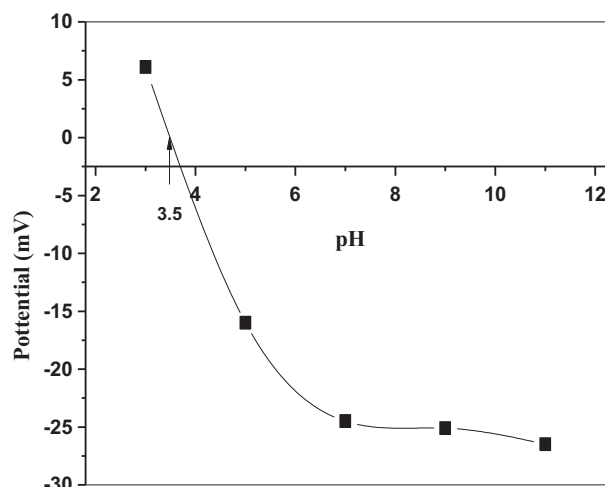


Fig. 4. Zeta potential measurement of the synthesized  $\text{NH}_2\text{-UiO-66}$ .

be attributed to the asymmetric and symmetric stretching of carboxyl functional groups, respectively [18,26]. An SEM image depicting the surface morphology of the synthesized material is shown in Fig. 3. From the image, an agglomeration of the uniform shaped particles with a size in the range of 14–16 nm can be observed. The zeta potential of  $\text{NH}_2\text{-UiO-66}$  is shown in Fig. 4 and the value of point of zero charge (pzc) was observed at a pH of 3.5. Above the zpc, the material was electropositive whereas below the zpc, it was electronegative. The BET surface area, pore size and pore volume of the synthesized material was found to be  $246.80\text{ m}^2/\text{g}$ ,  $0.019\text{ cc/g}$  and  $31.06\text{ \AA}$ , respectively.

#### 3.2. Effect of initial concentration of dye on adsorption

Initially, the effect of initial dye concentration (55 mg/L, 80 mg/L and 135 mg/L) on the adsorption capacity of the synthesized MOF was investigated. The amount of adsorbent in each batch experimental run was kept constant to 0.1 g/L and the experiments were carried out at a natural pH of the solution. Each experiment run was continued till a constant concentration of the dye was observed (which was attributed to the equilibrium concentration,  $C_e$ ). The amount of dye adsorbed on the adsorbent at different time,  $t$ , is calculated by Eq. (1). Fig. 5 shows a plot of  $q_t$  versus time for different initial concentrations of the dye solution. It was observed that for any initial concentration of the dye solution, the parameter

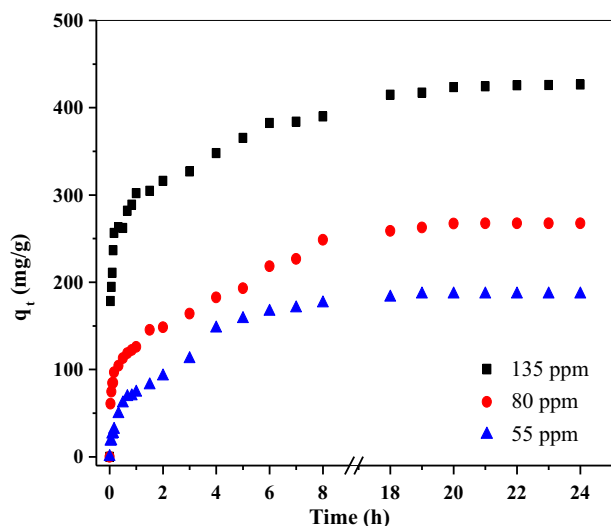


Fig. 5. Effect of initial concentration of dye on adsorption capacity of the synthesized  $\text{NH}_2\text{-UiO-66}$ .

$q_t$  increases rapidly in the initial 90 min of contact time. Between 90 and 480 min,  $q_t$  increases almost linearly with time and beyond 480 min, it remains constant till prolonged contact time. With the help of above experimental adsorption data, the value of  $q_e$  for different initial concentration of the dye solution viz. 55 mg/L, 80 mg/L and 135 mg/L was estimated as 177 mg/g, 248 mg/g and 390 mg/g, respectively.

In literature, the adsorption of Safranin dye is studied using different adsorbents. Table SI 1 (see supporting information) present list of materials reported for the adsorptive removal of safranin dye. From the table it can be seen that activated carbon and clay are mostly reported materials with an adsorption capacity as high as 1428.57 mg/g. In one of the recent publication by Adebowale et al. [28], the values of adsorption capacities of different adsorbents for the removal of the Safranin dye are compared. In comparison to the literature, adsorption capacity of synthesized  $\text{NH}_2\text{-UiO-66}$  observed in the present study (390 mg/g) is second best, among the reported adsorbents.

Supplementary data associated with this article can be found, in the online version, at <https://doi.org/10.1016/j.apt.2018.07.010>.

### 3.3. Effect of pH

Solution pH plays an important role in the adsorption process. The pH of the as-prepared Safranin dye solution with an initial concentration of 55–135 mg/L was found to be  $7.08 \pm 0.02$ .

Fig. 6 show the effect of pH on the adsorption capacity synthesized MOF for the removal of Safranin dye. The experimental adsorption data showed very similar patterns to that observed with changing the initial concentration of the dye solution. A rapid increase in  $q_t$  in the beginning till 90 min was followed by a linear increase between 90 and 480 min and thereafter remained constant till prolong time.

From the data, the values of  $q_e$  for the solution with pH of 4, 7 and 9 was observed to be 332 mg/g, 384 mg/g and 390 mg/g. Thus, a maximum adsorption at neutral pH was observed. From the zeta potential measurements of  $\text{NH}_2\text{-UiO-66}$  (Fig. 4), a zpc (point of zero charge) was observed at a pH of 3.5. Therefore, at any pH value above 3.5, the MOF was negatively charged whereas, at any pH value below 3.5, the MOF was positively charged. Since Safranin is a cationic dye, increasing the pH of the solution from 4 to 7 favoured the electrostatic interaction between dye molecules and

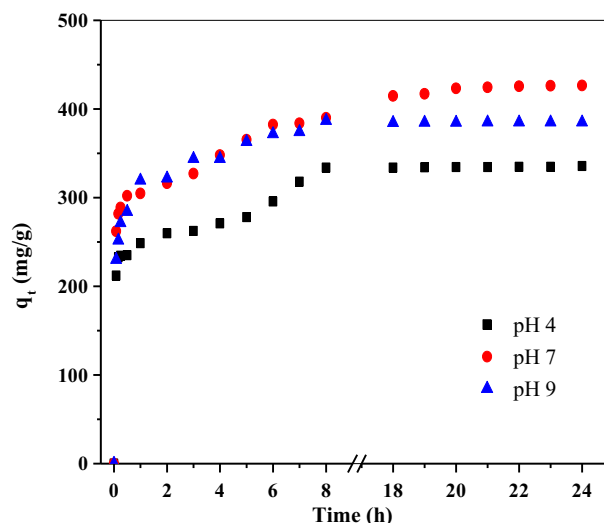


Fig. 6. Effect of pH of dye on adsorption capacity of the synthesized  $\text{NH}_2\text{-UiO-66}$ .

the adsorbent and thereby resulted into increased adsorption capacity of the material. Whereas, when the solution pH was further increased from 7 to 9, the adsorption capacity did not increase significantly due to the similar surface charges on the material as observed from the zeta potential.

In a study reported on the removal of Safranin basic dye onto the corncob activated carbon (with a zpc of 2.5), a maximum adsorption capacity is reported with a solution pH in the range of 5–9 [11]. In another study by Chen and co-worker, the zeta potential of  $\text{NH}_2\text{-UiO-66}$  was observed to be more electronegative ( $-4.91$  mV) than  $\text{UiO-66}$  ( $-3.65$  mV) and thus the former material showed better affinity towards cationic dyes [6]. The above study also concluded that the side group  $-\text{NH}_2$  captures proton and yield  $-\text{NH}_3^+$  thus, leading to efficient dye adsorbent onto the  $\text{NH}_2\text{-UiO-66}$  surface [6]. Thus, it can be concluded that the electronegative surface charges helps in efficient dye adsorption and the presence of  $-\text{NH}_2$  group further help in proton exchange of the adsorbed cationic dye molecules which enhances the overall process efficiency.

In the present work, the observed value of maximum adsorption capacity at neutral pH is in agreement with the literature. The study, therefore, suggests that the treatment can be employed without addition of any other chemicals (in order to change the pH).

At optimum conditions (initial dye concentration of 135 mg/L and as-prepared pH), the adsorption performance of  $\text{NH}_2\text{-UiO-66}$  was also compared with pristine  $\text{UiO-66}$  and the results are shown in Fig. 7. The dye adsorption onto  $\text{NH}_2\text{-UiO-66}$  was observed to be superior compared to  $\text{UiO-66}$ . As described earlier, the higher adsorption onto  $\text{NH}_2\text{-UiO-66}$  is attributed to the favorable electrostatic interactions between the adsorbents and cationic dyes. The observations are also in agreement with the earlier report [6].

### 3.4. Adsorption isotherms

In the present study, the experimental batch adsorption data was examined to fit with Langmuir, Freundlich, or Temkin adsorption isotherm models. The applicability of the isotherm models to the experimental batch adsorption data was decided based on the correlation coefficient ( $R^2$ ) of the linear fit.

The Langmuir isotherm assumes monolayer adsorption onto a surface containing a finite number of adsorption sites and is expressed as:

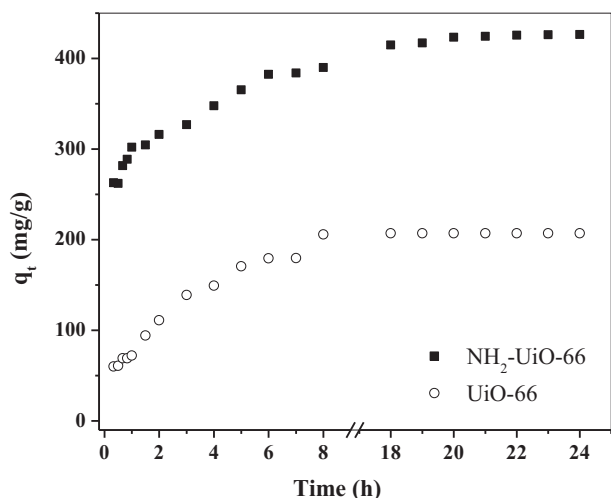


Fig. 7. Adsorption performance comparison between  $\text{NH}_2\text{-UiO-66}$  and pristine  $\text{UiO-66}$ .

$$\frac{C_e}{q_e} = \frac{1}{q_m K_L} + \frac{C_e}{q_m} \quad (3)$$

where  $C_e$  is the equilibrium concentration of the dye (mg/L),  $q_e$  is the amount of adsorption at equilibrium (mg/g),  $q_m$  is the theoretical maximum adsorption capacity (mg/g) and  $K_L$  is the Langmuir constant (L/mg) related to rate of adsorption. The values of  $q_m$  and  $K_L$  can be found out from a graph of  $C_e/q_e$  versus  $C_e$ . To confirm the favorability of the adsorption, the separation factor ( $R_L$ ) was calculated as:

$$R_L = \frac{1}{1 + C_0 K_L} \quad (4)$$

Where  $C_0$  is the initial dye concentration (mg/L). The value of  $R_L$  between 0 and 1 indicates favourable isotherm. For the present work, the values of  $q_m$  and  $K_L$  were found to be 1428.57 and 0.0038, respectively. However, the  $R^2$  (correlation coefficient) value of the graph of  $C_e/q_e$  versus  $C_e$  (Fig. SI 1, see supporting information) was 0.83. Further the value of separation factor ( $R_L$ ) for initial dye concentration of 55 mg/L, 80 mg/L and 135 mg/L, calculated using Eq. (4), was found to be 0.826, 0.765 and 0.659, respectively which indicates a favourable adsorption.

Freundlich adsorption isotherm is used to describe the adsorption characteristics for more than one monolayer coverage of the surface. A logarithmic form of Freundlich adsorption isotherm is shown in Eq. (6):

$$\ln q_e = \ln K_F + \frac{1}{n} \ln C_e \quad (5)$$

Where  $q_e$  and  $C_e$  has the same meaning as in Eq. (3).  $K_F$  and  $n$  are the Freundlich constants indicating favourability of the adsorption process and adsorption capacity of the adsorbent, respectively and can be found out by plotting a graph of  $\ln q_e$  versus  $\ln C_e$ . The values of  $K_F$  and  $n$  for the current data (calculated using Fig. SI 2, see supporting information) were found to be 2.235 and 0.436, respectively. In addition, the  $R^2$  value of the fit (Fig. SI 2, see supporting information) was observed as 0.99 indicating a good fit.

The Temkin isotherm describes the effect of indirect adsorbate/adsorbate interactions on the adsorption isotherm. It assumes that the heat of adsorption of all the molecules in the layer decreases linearly with coverage. A linearized form of Temkin isotherm is given by following equation:

$$q_e = \frac{RT}{K_T} \ln A_T + \left(\frac{RT}{K_T}\right) \ln C_e \quad (6)$$

Where  $q_e$  and  $C_e$  has the same meaning as in Eq. (3),  $A_T$  is the equilibrium binding constant,  $K_T$  is the constant related to the variation of adsorption energy,  $R$  the universal gas constant,  $T$  is the absolute temperature in K. The isotherm constants,  $A_T$  and  $K_T$  can be calculated from a plot of  $q_e$  versus  $\ln C_e$ . The values of isotherm constants  $A_T$  and  $K_T$  (calculated using Fig. SI 3, see supporting information) were found to be 0.060 and 11.61, respectively. In addition, the  $R^2$  value of the fit (Fig. SI 3, see supporting information) was observed as 0.96 indicating a good fit.

Table 1 summarizes the equilibrium constants of different isotherms along with the value of correlation coefficient of a linearized model fit. From this, it can be concluded that the experimental batch adsorption data follow Freundlich isotherm.

### 3.5. Adsorption kinetics

The experimental batch adsorption data was fitted to pseudo first-order and pseudo second-order kinetic model represented by Eqs. (7) and (8), respectively.

$$\ln(q_e - q_t) = \ln q_e - k_1 t \quad (7)$$

$$\frac{t}{q_t} = \frac{1}{k_2 q_e^2} + \frac{t}{q_e} \quad (8)$$

In above Eqs. (7) and (8),  $q_e$  and  $q_t$  are the amounts of dye adsorbed on the adsorbent (mg/g) at equilibrium and time  $t$ , respectively.  $k_1$  (1/h) and  $k_2$  (g/mg·h) are the rate constants of the pseudo first-order and pseudo second-order adsorption kinetic model, respectively. The parameters  $q_e$  and  $k_1$ , in the pseudo first-order model was estimated from a graph of  $\ln(q_e - q_t)$  versus  $t$  (Fig. 8a) as 185.47 mg/g and 0.469  $\text{h}^{-1}$ , respectively. Moreover, the correlation coefficient ( $R^2$ ) for the linear fit in Fig. 8a was 0.93. The parameters  $q_e$  and  $k_2$  in the pseudo second-order model estimated from a graph of  $t/q_t$  versus  $t$  (Fig. 8b) were found to be 384.61 mg/g and 0.014 g/mg·h, respectively. The correlation coefficient ( $R^2$ ) for the linear fit in this case was observed as 0.99. Furthermore, the value of  $q_e$  estimated by pseudo second-order kinetic model shows a better match with  $q_e$  obtained experimentally, compared to pseudo first-order kinetic model. Thus, on the basis of above observations, it can be concluded that the experimental batch adsorption data followed pseudo second-order kinetics.

Chen et al. reported a similar observation for adsorptive removal of methylene blue and methyl orange using  $\text{NH}_2\text{-UiO-66}$  [6]. In comparison to this, the rate constant as well as maximum adsorption capacity are observed to be much superior in the present work. Apart from this single study reported by Chen and coworkers, there are no reports in the literature on the kinetics of dye adsorption onto  $\text{NH}_2\text{-UiO-66}$ .

Table 1

Equilibrium constants of different isotherms for Safranin dye adsorption onto the synthesized MOF (pH of the dye solution = natural,  $7.08 \pm 2$ ; temperature: room temperature).

Langmuir isotherm			Freundlich isotherm			Temkin isotherm		
$q_m$	$K_L$	$R^2$	$n$	$K_F$	$R^2$	$A_T$	$K_T$	$R^2$
1428.57	0.0038	0.830	0.436	2.235	0.994	0.060	11.61	0.967

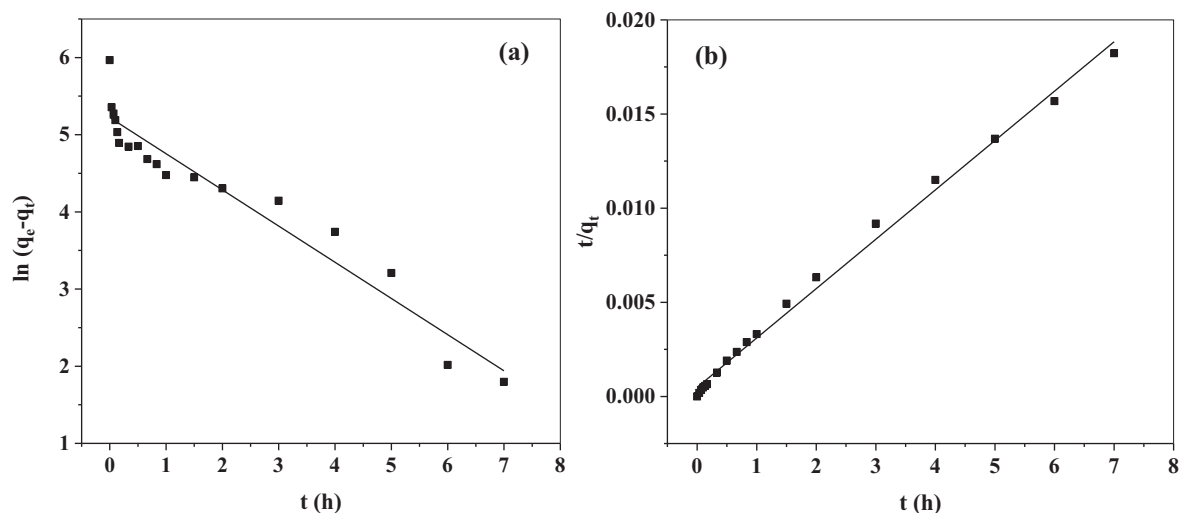


**Fig. 8.** A graph of (a)  $\ln (q_e - q_t)$  versus  $t$  to test the pseudo first-order model and (b)  $t/q_t$  versus  $t$  to test the pseudo second-order kinetic model fit to the experimental batch adsorption data.

### 3.6. Mechanism of adsorption

**Fig. 9** compares the FTIR spectra of fresh  $\text{NH}_2\text{-UiO-66}$  with the spent (after adsorption) material. In the FTIR spectra of spent material, two distinct peaks at  $1564\text{ cm}^{-1}$  and  $1378\text{ cm}^{-1}$  were observed similar to the fresh material. However, the other three distinct peaks at  $3452\text{ cm}^{-1}$ ,  $3348\text{ cm}^{-1}$  and  $2988\text{ cm}^{-1}$  which were present in case of fresh material, were replaced by a broad peak at  $3428\text{ cm}^{-1}$  and the same is attributed to the hydrogen bonded N-H stretch [29]. The broad peak at  $3428\text{ cm}^{-1}$  clearly indicates the hydrogen bonding between the dye molecule and the MOF [6].

### 3.7. Regeneration study

The techno-economic efficacy of MOFs is directly related to its reuse for multiple adsorption cycles. Therefore, in order to check

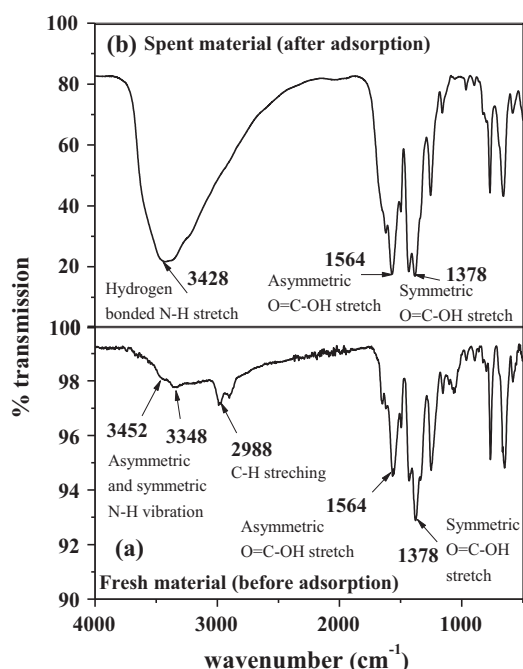


**Fig. 9.** FTIR spectrum of (a) fresh and (b) spent  $\text{NH}_2\text{-UiO-66}$ .

the stability of the MOF, regeneration and reuse studies were conducted. In this, the spent MOF material was recovered by filtration, washed with deionised water and dried at  $120\text{ }^\circ\text{C}$ . The material was then regenerated by washing with  $0.01\text{ N}$  sodium hydroxide and dried. The regenerated MOF was reused in the next adsorption cycle. **Fig. 10** shows the regeneration efficiency of  $\text{NH}_2\text{-UiO-66}$  after a few cycles of regeneration. It was observed even after 3 adsorption cycles, the regeneration efficiency was significant (above 90%). The result confirms that the  $\text{NH}_2\text{-UiO-66}$  MOF can be regenerated and reused multiple times.

### 3.8. Comparison with literature

Table SI 2 (see supporting information) present list of MOFs reported for the removal of dye effluents. From the table, it can be noted that Amino-MIL-101(Al) is reported to possess a maximum dye adsorption capacity of  $1409\text{ mg/g}$  at a solution temperature of  $50\text{ }^\circ\text{C}$ . However, the material is reported as a very poor sorbent upon reuse [30]. Further, materials such as MIL 100(Fe) have shown to possess an adsorption capacity of  $485\text{ mg/g}$  at a solution temperature of  $50\text{ }^\circ\text{C}$  [31]. However, near room temperature ( $35\text{ }^\circ\text{C}$ ), the

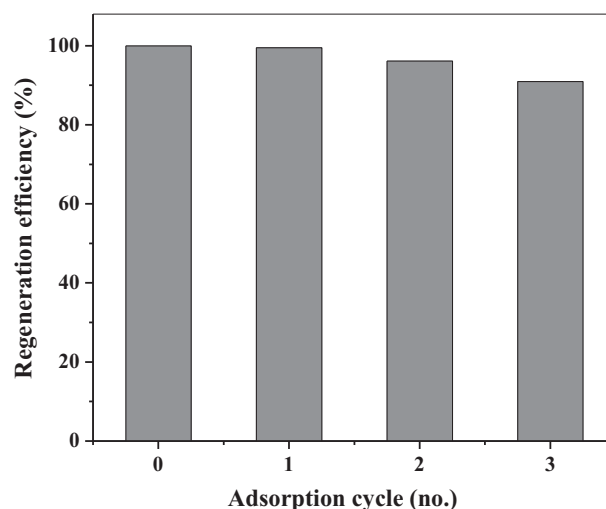


**Fig. 10.** Regeneration and reusability study of adsorptive removal of safranin dye using  $\text{NH}_2\text{-UiO-66}$ .

adsorption capacity of the same material is observed as 325 mg/g [31]. In another study by Haque and co-worker MOF-235 is shown to possess a maximum methyl orange adsorption capacity of 448 mg/g at near room temperature (35 °C) and 501 mg/g at a solution temperature of 45 °C [32]. However, the reported values are at acidic pH conditions (pH = 4) and the dye adsorption capacity of the reported materials at neutral pH conditions is about 370 mg/g [32]. More recently, Embaby and coworkers reported a record adsorption capacity of 400 mg/g for the removal of Alizarin Red S with UiO-66 [21]. However, the high efficiency is observed at a low dye concentration of 11.82 ppm and at highly acidic conditions (solution pH = 2). Such extreme acidic conditions of pH values of 2 and 4 are techno-economically unfavorable for environmental applications. Therefore, in comparison to the above reported literature till data, the observed dye adsorption capacity of 390 mg/g at normal room temperature and near natural pH of the dye solution in the present study is much superior technically as well as economically.

#### 4. Conclusion

In the present study, NH<sub>2</sub>-UiO-66 was synthesized by hydrothermal synthesis. The synthesized material was observed to be crystalline with a size of 15 ± 2 nm and BET surface area of 246.80 m<sup>2</sup>/g. As an application part, the material was used as an adsorbent for the removal of Safranin dye. From the batch adsorption experiments, the value of q<sub>e</sub> for different initial concentration of the dye solution viz. 55 mg/L, 80 mg/L and 135 mg/L was estimated as 177 mg/g, 248 mg/g and 390 mg/g, respectively. A maximum dye adsorption was observed at a neutral pH of the solution. Comparison of NH<sub>2</sub>-UiO-66 with pristine UiO-66 showed the former as a superior adsorbent. The FTIR study of the fresh and spent material revealed that formation of hydrogen bonding between the dye molecule and the NH<sub>2</sub>-UiO-66 as a possible mechanism of superior adsorption onto its surface. The experimental batch adsorption data followed Freundlich adsorption isotherm and pseudo second order kinetics. The regeneration study indicated that the NH<sub>2</sub>-UiO-66 can be reused multiple times without significant loss in its efficiency. The observed dye adsorption capacity is much superior technically as well as economically, compared to earlier reports in the literature. Thus, NH<sub>2</sub>-UiO-66 has a strong potential as an alternative adsorbent.

#### Acknowledgements

Financial support from DST INSPIRE research grant (IFA-13-ENG-59) is gratefully acknowledged.

#### References

- [1] S. Lin, Z. Song, G. Che, A. Ren, P. Li, C. Liu, J. Zhang, Adsorption behavior of metal-organic frameworks for methylene blue from aqueous solution, *Micropor. Mesopor. Mater.* 93 (2014) 27–34.
- [2] M. Sarker, J.Y. Song, S.H. Jung, Adsorptive removal of anti-inflammatory drugs from water using graphene oxide/metal-organic framework composites, *Chem. Eng. J.* 335 (2018) 74–81.
- [3] N.A. Khan, Z. Hasan, S.H. Jung, Adsorptive removal of hazardous materials using metal-organic frameworks (MOFs): a review, *J. Hazard. Mater.* 244–245 (2013) 444–456.
- [4] Z. Hasan, S.H. Jung, Removal of hazardous organics from water using metal-organic frameworks (MOFs): plausible mechanisms for selective adsorptions, *J. Hazard. Mater.* 283 (2015) 329–339.
- [5] G.E. Cmarik, M. Kim, S.M. Cohen, K.S. Walton, Tuning the adsorption properties of UiO-66 via ligand functionalization, *Langmuir* 28 (44) (2012) 15606–15613.
- [6] Q. Chen, Q. He, M. Lv, Y. Xu, H. Yang, X. Liu, F. Wei, Selective adsorption of cationic dyes by UiO-66-NH<sub>2</sub>, *Appl. Surf. Sci.* 327 (2015) 77–85.
- [7] K.-Y.A. Lin, Y.-T. Liu, S.-Y. Chen, Adsorption of fluoride to UiO-66-NH<sub>2</sub> in water: stability, kinetic, isotherm and thermodynamic studies, *J. Colloid Interface Sci.* 461 (2016) 79–87.
- [8] Y. Li, Y. Liu, W. Gao, L. Zhang, W. Liu, J. Lu, Z. Wang, Y.-J. Deng, Microwave-assisted synthesis of UiO-66 and its adsorption performance towards dyes, *CrystEngComm* 16 (2014) 7037–7042.
- [9] R. Malik, D.S. Ramteke, S.R. Wate, Adsorption of malachite green on groundnut shell waste based powdered activated carbon, *Waste Manage. (Oxford)* 27 (9) (2007) 1129–1138.
- [10] T. Robinson, G. McMullan, R. Marchant, P. Nigam, Remediation of dyes in textile effluent: a critical review on current treatment technologies with a proposed alternative, *Bioresour. Technol.* 77 (2001) 247–255.
- [11] S. Preethi, A. Sivasamy, S. Sivasenan, V. Ramamurthi, G. Swaminathan, Removal of safranin basic dye from aqueous solutions by adsorption onto corn cob activated carbon, *Ind. Eng. Chem. Res.* 45 (2006) 7627–7632.
- [12] K. Kadirvelu, M. Kavipriya, C. Karthika, M. Radhika, N. Vennilamani, S. Pattabhi, Utilization of various agricultural wastes for activated carbon preparation and application for the removal of dyes and metal ions from aqueous solutions, *Bioresour. Technol.* 87 (2003) 129–132.
- [13] G. Crini, Non-conventional low-cost adsorbents for dye removal: a review, *Bioresour. Technol.* 97 (2006) 1061–1085.
- [14] S.-F. Kang, C.-H. Liao, S.-T. Po, Decolorization of textile wastewater by photo-Fenton oxidation technology, *Chemosphere* 41 (2000) 1287–1294.
- [15] B. dos Santos, F.J. Cervantes, J.B. van Lier, Review paper on current technologies for decolourisation of textile wastewaters: perspectives for anaerobic biotechnology, *Bioresour. Technol.* 98 (2007) 2369–2385.
- [16] S. Tambat, S. Umale, S. Sontakke, Photocatalytic degradation of Milling Yellow dye using sol-gel synthesized CeO<sub>2</sub>, *Mater. Res. Bull.* 76 (2016) 466–472.
- [17] Y. Qiu, Z. Zheng, Z. Zhou, G.D. Sheng, Effectiveness and mechanisms of dye adsorption on a straw-based biochar, *Bioresour. Technol.* 100 (21) (2009) 5348–5351.
- [18] H. Molavi, A. Eskandari, A. Shojaei, S.A. Mousavi, Enhancing CO<sub>2</sub>/N<sub>2</sub> adsorption selectivity via post-synthetic modification of NH<sub>2</sub>-UiO-66 (Zr), *Micropor. Mesopor. Mater.* 257 (2018) 193–201.
- [19] Q. He, Q. Chen, M. Lü, X. Liu, Adsorption behavior of Rhodamine B on UiO-66, *Chin. J. Chem. Eng.* 22 (11–12) (2014) 1285–1290.
- [20] K.-D. Zhang, F.-C. Tsai, N. Ma, Y. Xia, H.-L. Liu, X.-Q. Zhan, X.-Y. Yu, X.-Z. Zeng, T. Jiang, D. Shi, C.-J. Chang, Adsorption behavior of high stable Zr-based MOFs for the removal of acid organic dye from water, *Materials* 10 (2) (2017) 205.
- [21] M.S. Embaby, S.D. Elwany, W. Setyaningsih, M.R. Saber, The adsorptive properties of UiO-66 towards organic dyes: a record adsorption capacity for the anionic dye Alizarin Red S, *Chin. J. Chem. Eng.* 26 (4) (2018) 731–739.
- [22] W. Zhang, H. Huang, C. Zhong, D. Liu, Cooperative effect of temperature and linker functionality on CO<sub>2</sub> capture from industrial gas mixtures in metal-organic frameworks: a combined experimental and molecular simulation study, *PCCP* 14 (2012) 2317–2325.
- [23] J.H. Cavka, S. Jakobsen, U. Olsbye, N. Guillou, C. Lamberti, S. Bordiga, K.P. Lillerud, A new zirconium inorganic building brick forming metal organic frameworks with exceptional stability, *J. Am. Chem. Soc.* 130 (42) (2008) 13850–13851.
- [24] L. Shen, W. Wu, R. Liang, R. Lin, L. Wu, Highly dispersed palladium nanoparticles anchored on UiO-66(NH<sub>2</sub>) metal-organic framework as a reusable and dual functional visible-light driven photocatalyst, *Nanoscale* 5 (19) (2013) 9374–9382.
- [25] C.L. Luu, T.T.V. Nguyen, T. Nguyen, T.C. Hoang, Synthesis, characterization and adsorption ability of UiO-66-NH<sub>2</sub>, *Adv. Nat. Sci.: Nanosci. Nanotechnol.* 6 (2015), 025004(1–6).
- [26] J. Hou, Y. Luan, J. Tang, A.M. Wensley, M. Yang, Y. Lu, Synthesis of UiO-66-NH<sub>2</sub> derived heterogeneous copper (II) catalyst and study of its application in the selective aerobic oxidation of alcohols, *J. Mol. Catal. A: Chem.* 407 (2015) 53–59.
- [27] M. Mahdiani, A. Sobhani, F. Ansari, M.S. Niasari, Lead hexaferrite nanostructures: green amino acid sol-gel autocombustion synthesis, characterization and considering magnetic property, *J. Mater. Sci.: Mater. Electron.* 28 (2017) 17627–17634.
- [28] K.O. Adebowale, B.I. Olu-owolabi, E.C. Chigbundu, Removal of Safranin-O from aqueous solution by adsorption onto Kaolinite clay, *J. Encapsulation Adsorpt. Sci.* 4 (2014) 89–104.
- [29] M.K. Sahu, U.K. Sahu, R.K. Patel, Adsorption of safranin-O dye on CO<sub>2</sub> neutralized activated red mud waste: process modelling, analysis and optimization using statistical design, *RSC Adv.* 5 (2015) 42294–42304.
- [30] E. Haque, V. Lo, A.I. Minett, A.T. Harris, T.L. Church, Dichotomous adsorption behaviour of dyes on an amino-functionalised metal-organic framework, amino-MIL-101(Al), *J. Mater. Chem. A* 2 (1) (2014) 193–203.
- [31] S.-H. Huo, X.-P. Yan, Metal-organic framework MIL-100(Fe) for the adsorption of malachite green from aqueous solution, *J. Mater. Chem.* 22 (2012) 7449–7455.
- [32] E. Haque, J.W. Jun, S.H. Jung, Adsorptive removal of methyl orange and methylene blue from aqueous solution with a metal-organic framework material, iron terephthalate (MOF-235), *J. Hazard. Mater.* 185 (2011) 507–511.